AAEC/E 125

UNCLASSIFIED

AAEC/E 125

AUSTRALIAN ATOMIC ENERGY COMMISSION

RESEARCH ESTABLISHMENT

LUCAS HEIGHTS

FURTHER EXAMINATION OF IRRADIATED HOT-PRESSED BERYLLIUM OXIDE BASED FUEL SPECIMENS

by

G. L. HANNA

Issued Sydney, August 1964

UNCLASSIFIED

AUSTRALIAN ATOMIC ENERGY COMMISSION

RESEARCH ESTABLISHMENT

LUCAS HEIGHTS

FURTHER EXAMINATION OF IRRADIATED HOT-PRESSED BERYLLIUM OXIDE BASED FUEL SPECIMENS

by

G. L. HANNA

ABSTRACT

The work reported in AAEC/E106 on the metallographic examination of $(U,Th)O_2$ dispersed in BeO irradiated in a thermal neutron flux is extended. X-ray diffraction studies have demonstrated that strain developed in the matrixes of both coarse and fine dispersions during irradiation was more severe in the fine dispersion. It is thought that in the coarse dispersion it arose from the swelling of fuel particles and in the fine dispersion, from fission fragment damage. The strain was relieved by annealing in the range 1000 – 1350 °C and was partly relieved in the coarse dispersion by crushing.

Fission gas bubbles were observed in the microstructure of specimens annealed at 1250 °C and 1500 °C after irradiation.

CONTENTS

1. INTRODUCTION

In mid–1960, hot pressed specimens of urania–thoria solid solutions, $(U,Th)O_2$, dispersed in beryllium oxide were irradiated in Rig X – 12 in the Australian Atomic Energy Commission's reactor HIFAR. The examination of these specimens for dimension, density, and micro–structural changes and for fission gas releases was reported by Hanna, Hickman, and Hilditch (1963). The present report describes X–ray diffraction experiments and further metallographic examination of selected specimens which were annealed after irradiation.

2. EXPERIMENTAL

2.1 X–Ray Diffraction

The object of the X–ray diffraction examination was to examine the resultant lattice changes in specimens which were identical in all respects except the size of fuel particles. The specimens were selected from those having lowest uranium content and, hence, were the least radioactive. Extension of the examination to specimens of higher fission density was prevented by their high activity and the lack of suitably shielded apparatus.

Specimens were chosen so as to give a comparison of coarse particle dispersions in which the matrix was substantially undamaged by fission fragments and fine particle dispersions in which the whole matrix was damaged. The specimens used were Nos. 106 and 107, (100 to 185 micron fuel particles) in which, according to theory (White, Beard, and Willis 1957 and Weber, 1959), only 3.3 per cent. of the matrix should have been damaged, and Nos. 148 and 149 (0 to 50 micron fuel particles) in which the whole matrix should have been damaged. All specimens contained 4.4 volume per cent. of $(U,Th)O_2$ in which the fissile to fertile ratio was 8 : 23.

Specimens 107 and 149 were used to obtain diffraction profiles of the as–irradiated material. Two discs 1 cm diameter and 4 mm thick were cut from each of specimens 106 and 148; one disc from each specimen was crushed to powder of minus 150 micron particle size and the others were examined after one hour anneals at 800, 1000, 1200, and 1350°C.

Diffraction profiles were obtained with a Siemens diffractometer using a proportional counter and pulse height discrimination. Using Cu Kα radiation, profiles from specimens 107, 149, and the two crushed discs were recorded over the range θ = 12° to θ = 82° at a scanning rate of 1/8° per minute. Step scanning was used to obtain accurate profiles of the BeO 30.0, 21.0, and 20.3 reflections and the $(U,Th)O_2$ 531 and 622 reflections from specimens 107, 149, 110, 152, and all annealed specimens. Cobalt radiation was used to record the BeO 20.3 and $(U,Th)O_2$ 531 reflections and copper radiation was used for all other reflections.

2.2 Metallography

Specimens 102, 120, 141, and 153 were chosen for annealing and metallographic examination. Their compositions are given in Table 1 together with the fission densities of both whole specimens and the fuel material alone. Specimen 153 contained fine fuel particles (0 – 50 microns) and all others contained coarse particles (100 – 185 microns).

Three discs of 0.9 cm diameter and 4 mm thick were cut from each specimen; one was annealed for one hour at 1000°C, one at 1250°C, and one at 1500°C. Annealed specimens were mounted in epoxy resin, ground on 120 through to 600 grit papers and polished for 48 hours on a vibratory polishing machine using medium grade alumina in ethylene glycol. Specimens were examined in the unetched condition.

Control samples of unirradiated material were annealed and polished with the irradiated specimens in the high activity handling cells.

3. RESULTS

3.1 X–Ray Diffraction

The investigation of line shifts and line broadening was complicated by the overlapping of certain $(U,Th)O_2$ and BeO reflections and the extent of the broadening which in many cases prevented the resolution of the $\alpha_1 - \alpha_2$ doublets. The interference of reflections was more troublesome in the fine dispersion where the $(U,Th)O_2$ reflections were more intense; reflections where overlapping occurred are indicated in Table 2.

The results may be summarised as follows:

(i) All reflections present in the unirradiated materials were still visible after irradiation but considerable broadening of both BeO and $(U,Th)O_2$ reflections occurred. The effects were more marked in the fine dispersion (specimens 148 and 149) where no $\alpha_1 - \alpha_2$ doublets could be resolved within the angular range of the diffractometer (θ = 0 to θ = 82°). With the coarse dispersions (numbers 106 and 107) doublets could be resolved at $\theta \geqslant 60°$ compared with $\theta \geqslant 35°$ in the unirradiated material. Measurements of line–broadening are given in Table 2.

(ii) No shifts in peak positions could be detected in the coarse dispersion material and the lines from the fine dispersion were too diffuse for reliable measurement of peak positions.

(iii) Measurements of line breadths in the coarse dispersion samples showed that the broadening was least for h,k,O reflections, was greater for h,k,l reflections, and increased with increasing l.

(iv) Crushing the samples relieved considerably the broadening of many BeO reflections from the coarse dispersion (see Table 2) but made no change in the reflections from the fine dispersion.

(v) Annealing of massive samples resulted in recovery of the broadening of all BeO reflections from the coarse dispersion, commencing after 1 hour at 1000°C and becoming complete after 1 hour at 1350°C. In fine dispersions, no recovery was apparent at 1000°C but recovery was complete at 1350°C. Broadening of $(U,Th)O_2$ reflections only partly recovered at 1350°C in both dispersions.

3.2 Metallography

Typical microstructures of specimens in the unirradiated and irradiated condition are shown in Figures 1(a) and 1(b). The following microstructural changes were observed in the annealed specimens:

1000°C

A noticeable decrease in the amount of grain pull–out in the matrixes of coarse dispersions. (Figure 2).

1250°C

A further decrease in the amount of grain pull–out in the matrixes of coarse dispersions and a distribution of fine rounded pores in the grain boundaries of most fuel particles (Figure 3). Those particles which did not contain grain boundary pores were free from fabrication pores and inclusions. Pores within grains were very infrequent at this stage.

1500°C

(a) Coarse dispersions: Grain pull–out was eliminated and matrix porosity was comparable with that in unirradiated material. The delineation of fuel particle grains was very pronounced and pores were generally observed within grains (Figures 4(a) and 4(b)). The density and size of pores in particles at the specimens' surfaces were noticeably greater than in particles away from the surface (Figure 5). Pores were sometimes seen at fuel – BeO interfaces and in BeO grain boundaries which intersected the interfaces.

(b) Fine dispersion: There was a uniform distribution of pores in the BeO grain boundaries and at fuel – BeO interfaces (Figure 6). There was no evidence of pores within the fuel particles of the BeO grains.

Control samples annealed with the irradiated samples sometimes tended to develop similar distributions of porosity. This was particularly so in specimen 120 but in all other control specimens the pore density was always far less than in irradiated specimens.

4. DISCUSSION

Perhaps the most interesting X-ray result was the broadening of reflections from the BeO matrix of the coarse dispersion. The theory of dispersion fuels developed by White, Beard, and Willis (1957) appears sufficiently well founded to rule out fission fragment bombardment as the major cause of the line broadening. However, the dependence of the value of $\beta \cot \theta$ (Table 2) on the reflection indices indicates that lattice defects did contribute to the broadening. The only other source of lattice defects would be fast neutron bombardment. The fast neutron dose arising from the reactor flux should not have exceeded 2×10^{18} nvt which is too low to cause measurable line broadening in BeO. However, the effective dose derived from the fission neutrons produced within the specimens themselves can be calculated from the work of Lawrence (1963) to be about 7×10^{19} nvt. Reference to the data given by Hickman (1962) for neutron irradiated BeO shows that this is high enough to give the observed broadening of the 20.3 reflection from specimen 107 (0.3 degrees of θ) but cannot account for the high 30.0 broadening (expected to be about 0.05 degrees of θ) and the insignificant shift in the 20.3 reflection (expected to be about 1 degree of θ).

Partial relief of the broadening of the 30.0, 21.2, 21.1, 21.0, 20.2, and 20.1 reflections (see Table 2) by crushing specimen 106 suggests that much of the broadening and lattice strain may have been due to stresses imposed by the swelling of fuel particles. Unfortunately the irregular shape and uneven surfaces of fuel particles make it impossible to measure by quantitative metallography the small, irradiation-induced differences in the true volume fraction of fuel material.

The annealing experiments were too limited to assist in explaining the X-ray line broadening since recovery occurred in the range 1000 – 1350 °C. The annealing results can be explained by both defect annealing and stress relaxation by creep.

The reduction of grain pull-out by annealing after irradiation is consistent with the recovery of X-ray line broadening and is indicative of the relief of strain in the matrix. The appearance of fine rounded pores in the fuel material is undoubtedly due to fission gas precipitation and the annealing experiments suggest that bubble formation during irradiation at low burn-ups may not be significant at temperatures below about 1200 °C. This is, perhaps, an optimistic inference in view of the short annealing time but it appears to be supported by the work of Johnson and Lofftus (1962) whose photomicrographs did not show bubble formation at 1200 °C and 2.5×10^{21} fissions per cm^3 of UO_2 and of Johnson and Mills (1963) whose photomicrographs show grain boundary pores at 1310 °C and 6.6×10^{20} fissions per cm^3 of UO_2. One cannot assume however, that this situation would persist to higher burnups because Barney and Wemple (1958), Bleiberg et al. (1960) and Yeniscavich and Bleiberg (1960) have shown that structural changes occurring in UO_2 at 1.5 to 2.5×10^{21} fissions per cm^3 allow gas bubbles to form readily even at low temperatures.

The preferential formation of gas bubbles at grain boundaries and within grains containing pores and inclusions suggests that nucleation is probably heterogeneous and may be suppressed in high density, high purity material. The greater ease of bubble formation and the swelling of these particles at the unrestrained faces was similar to the behaviour of specimens irradiated by Barney and Wemple (1958). However, despite the short annealing time it is doubtful whether the material had the same plasticity as the UO_2 of Barney and Wemple in which swelling occurred at temperatures as low as 200 °C during irradiation.

The dimension changes reported by Hanna et al. (1963) showed that the radiation resistance of fine dispersions was likely to be inferior to that of coarse dispersions. The severe X-ray line broadening observed with the fine dispersions is consistent with this conclusion and is evidence of the greater matrix damage arising from the use of fine fuel particles. As stated in Section 2.1, dispersion fuel theory predicts that all the matrix in the fine dispersions will be exposed to fission fragment bombardment compared with only 3.3 per cent. in the coarse dispersion. Furthermore, it can be shown (Equation 1 in the paper by Weber (1959)) that about 50 per cent. of the fission products escaped from the fine fuel particles used in these experiments and consequently, fuel particles should not have swollen. Hence, the X-ray line broadening was probably due entirely to particle bombardment and, in particular, to fission fragment bombardment.

The formation of fission gas bubbles within the matrix during post-irradiation annealing (Figure 6) is additional evidence of extensive matrix damage in the fine dispersion.

5. CONCLUSION

X-ray diffraction studies have demonstrated that strain develops at relatively low burn-ups in the matrixes of both fine and coarse dispersions of $(U,Th)O_2$ in BeO and that the effect is more pronounced in the fine dispersions. It appears probable that lattice defects were produced throughout the matrix of coarse dispersions despite the fact that the attempt was made to irradiate in a purely thermal neutron flux. It is not clear yet how these defects were produced. Much of the strain in coarse dispersions appears to result from stresses imposed by swollen fuel particles.

The formation of fission gas bubbles during post-irradiation annealing did not become significant until 1250 °C and nucleation appears to be heterogeneous. The results of other workers however, suggest that bubbles will form at lower temperatures at higher burn-ups.

6. ACKNOWLEDGMENTS

The author is grateful to Mr. B.S. Hickman for helpful discussion of the X-ray diffraction experiments and to Messrs. J. H. Meller and R.J. Starling who did the metallographic preparation and the annealing treatments.

7. REFERENCES

Barney, W.K., and Wemple, B.D. (1958). - KAPL - 1836.

Bleiberg, M.L., Mascarinec, G., Clark, D., and Yeniscavich, W. (1960). - WAPD - BT - 18.

Hanna, G.L., Hickman, B.S., and Hilditch, R.J. (1963). - AAEC/E106.

Hickman, B.S. (1962). - AAEC/E 99.

Johnson, D.E.,and Lofftus, F.H. (1962). - GA - 3483.

Johnson, D.E., and Mills, R.G. (1963). - GA - 4138.

Lawrence, B.R. (1963). - AAEC/TM213.

White, D.E., Beard, A.P., and Willis, A.H. (1957). - KAPL - 1909.

Weber, C.E. (1959). - Progress in Nuclear Energy, Series V, Volume 2 p.295. Pergamon Press, London.

Yeniscavich, W., and Bleiberg, M.L. (1960). - WAPD - BT - 20.

TABLE 1

SPECIMEN COMPOSITIONS AND FISSION DENSITIES

Specimen No.	Fuel Content v/o $(U,Th)O_2$	Molar Ratio $UO_2 : ThO_2$	Fuel Particle Size (microns)	Burn-up (a/o heavy metal)	Fission Density (fissions cm^{-3})	
					Whole Specimen	Fuel Material
102	3	8 : 23	100 – 185	3.4	2×10^{19}	7.5×10^{20}
106 107	4.4	8 : 23	100 – 185	3.5	3.5×10^{19}	8.0×10^{20}
120	15.7	8 : 23	100 – 185	3.0	1.0×10^{20}	6.5×10^{20}
141	4.4	25 : 6	100 – 185	7.5	8.0×10^{19}	1.8×10^{21}
148 149 153	4.4	8 : 23	0 – 50	3.1	3.0×10^{19}	7.0×10^{20}

TABLE 2

X-RAY LINE BROADENING MEASUREMENTS

	Specimen 106			Specimen 148		Remarks
	Broadening β, °θ	$\beta \cot \theta$	Recovery of β on Crushing %	Broadening β, °θ	$\beta \cot \theta$	
10.0	0.03	0.09	–	0.03	0.09	
00.2	0.1	0.25	–	0.05	0.15	
10.1	0.05	0.15	–	0.1	0.25	
10.2	0.15	0.25	–	–	–	Overlap with $(U,Th)O_2$ 222
11.0	0.07	0.1	–	0.2	0.3	
10.3	0.2	0.25	–			Overlap with $(U,Th)O_2$ 420
20.0	0.7	0.08				
11.2	0.2	0.2	12.5			
20.1	0.1	0.1	–			Slight overlap with $(U,Th)O_2$ 422
20.2	0.25	0.25	27			
20.3	0.35	0.2	–			
21.0	0.15	0.08	67			Overlap with $(U,Th)O_2$ 620
21.1	0.2	0.1	28			
11.4	–	–	–			Overlap with $(U,Th)O_2$ 533
21.2	0.6	0.22	42			
30.0	0.5	0.08	60			Slight overlap with $(U,Th)O_2$ 622

TABLE 3

X-RAY LINE BREADTHS OF ANNEALED SPECIMENS

Specimen No.	Treatment	X-ray Line Breadths, °θ		
		BeO 30.0	BeO 21.0	BeO 20.3
110	as fabricated	0.3	0.1	0.2
107	irradiated	0.65	0.25	diffuse
	annealed 800 °C	0.65	0.17	,,
	1000 °C	0.45	0.17	,,
	1200 °C	0.35	0.1	0.3
	1350 °C	0.25	0.1	0.22
152	as fabricated	0.4	0.1	0.25
148	irradiated	diffuse	diffuse	diffuse
	annealed 800 °C	,,	,,	,,
	1000 °C	,,	,,	,,
	1200 °C	0.6	0.12	0.3
	1350 °C	0.6	0.12	0.25

X 160

(a) As fabricated

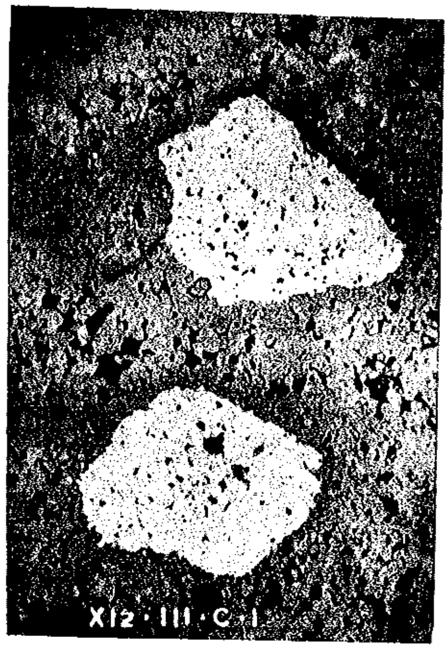

X 160

(b) As irradiated

FIGURE 1. TYPICAL MICROSTRUCTURES OF SPECIMENS BEFORE POST-IRRADIATION ANNEALING

X 160

FIGURE 2. MICROSTRUCTURE OF SPECIMEN 102 ANNEALED 1 HOUR AT 1000°C

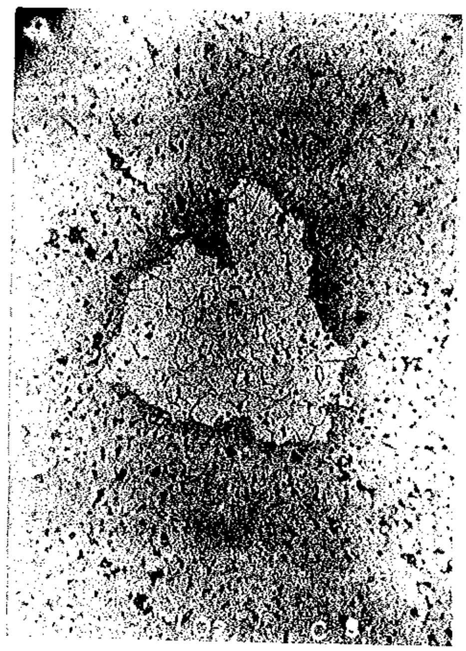

X 160

FIGURE 3. MICROSTRUCTURE OF SPECIMEN 102 ANNEALED 1 HOUR AT 1250°C

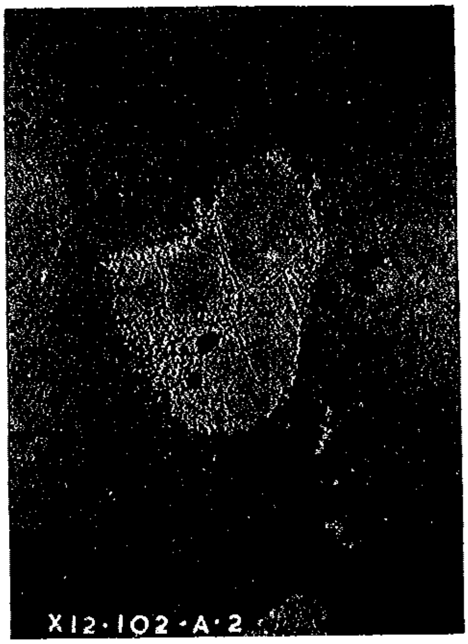

X 160

FIGURE 4(a) MICROSTRUCTURE OF SPECIMEN 102 ANNEALED 1 HOUR AT 1500 °C

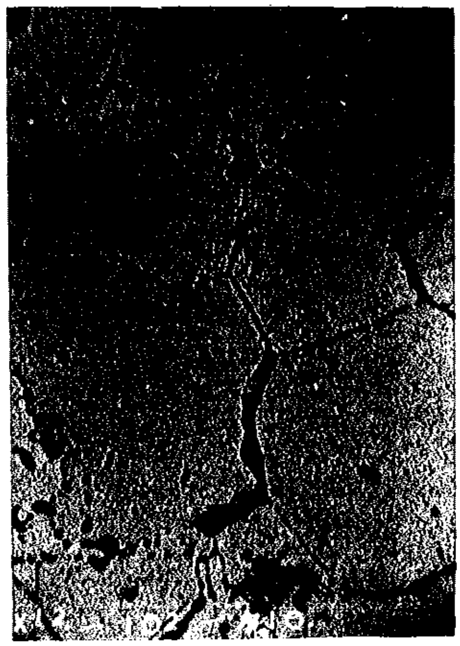

X 525

FIGURE 4(b) FISSION GAS BUBBLES IN A FUEL PARTICLE OF SPECIMEN 102 ANNEALED AT 1500° C

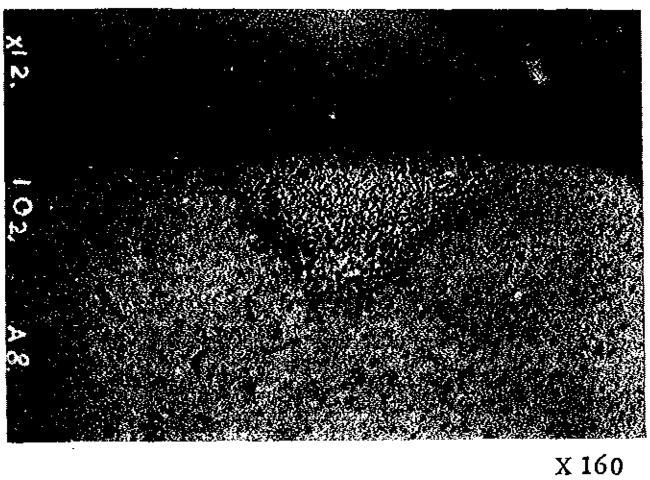

X 160

FIGURE 5. FISSION GAS BUBBLES IN A SURFACE FUEL PARTICLE OF SPECIMEN 102 ANNEALED AT 1500° C

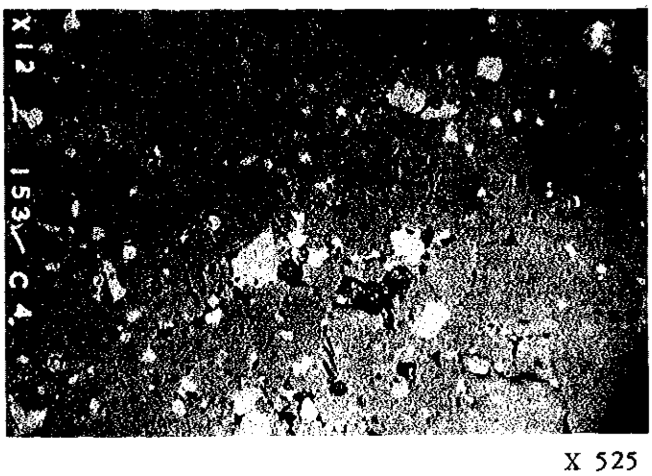

X 525

FIGURE 6. MICROSTRUCTURE OF THE FINE DISPERSION (SPECIMEN 153) ANNEALED FOR 1 HOUR AT 1500° C